

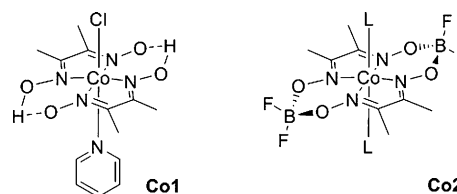
## Photocatalysis

Microsecond X-ray Absorption Spectroscopy Identification of Co<sup>I</sup> Intermediates in Cobaloxime-Catalyzed Hydrogen EvolutionGrigory Smolentsev,<sup>\*[a]</sup> Bianca Cecconi,<sup>[b, c]</sup> Alexander Guda,<sup>[d]</sup> Murielle Chavarot-Kerlidou,<sup>[b]</sup> Jeroen A. van Bokhoven,<sup>[a, e]</sup> Maarten Nachttegaal,<sup>[a]</sup> and Vincent Artero<sup>[b]</sup>

**Abstract:** Rational development of efficient photocatalytic systems for hydrogen production requires understanding the catalytic mechanism and detailed information about the structure of intermediates in the catalytic cycle. We demonstrate how time-resolved X-ray absorption spectroscopy in the microsecond time range can be used to identify such intermediates and to determine their local geometric structure. This method was used to obtain the solution structure of the Co<sup>I</sup> intermediate of cobaloxime, which is a non-noble metal catalyst for solar hydrogen production from water. Distances between cobalt and the nearest ligands including two solvent molecules and displacement of the cobalt atom out of plane formed by the planar ligands have been determined. Combining in situ X-ray absorption and UV/Vis data, we demonstrate how slight modification of the catalyst structure can lead to the formation of a catalytically inactive Co<sup>I</sup> state under similar conditions. Possible deactivation mechanisms are discussed.

Light-driven catalytic systems for hydrogen evolution from water are crucial components of our energy future.<sup>[1,2]</sup> Efficient photocatalytic hydrogen evolution systems contain platinum nanoparticles or other noble metals that are expensive and of limited availability. This has triggered the development of catalysts based on earth-abundant 3d elements, such as cobalt, iron, and nickel.<sup>[3–8]</sup> Cobaloximes are perspective and popular

hydrogen-evolving molecular catalysts<sup>[7–9]</sup> and they have been implemented in many homogeneous multicomponent photocatalytic systems.<sup>[7,10–16]</sup> The Co<sup>III</sup> complex [Co(dmgh)<sub>2</sub>pyCl] (**Co1**, dmgh<sub>2</sub> = dimethylglyoxime, py = pyridine Scheme 1) with



**Scheme 1.** Structure of cobaloxime catalysts **Co1** and **Co2** (L = H<sub>2</sub>O or CH<sub>3</sub>CN).

proton bridges between dmgh<sup>2-</sup> ligands and the Co<sup>II</sup> complex [Co(dmghBF<sub>2</sub>)<sub>2</sub>L<sub>2</sub>] (**Co2**, L = H<sub>2</sub>O or CH<sub>3</sub>CN) with {BF<sub>2</sub>} bridges are the two most-studied cobaloxime platforms so far. Rational optimization of such systems, however, depends on our understanding of the cobalt-based catalytic cycle, including the electronic and geometric structure of intermediates along the catalytic cycle and the possible routes that lead to deactivation.

Different reaction mechanisms for hydrogen evolution have been proposed that involve homolysis<sup>[14,17,18]</sup> or protonation of a cobalt–hydride bond<sup>[17,19,20]</sup> They all involve a primary Co<sup>I</sup> intermediate which is then protonated to yield a Co<sup>III</sup>H hydride species. Such a Co<sup>I</sup> intermediate has been observed for an analogue of **Co2**, [Co(dpgBF<sub>2</sub>)<sub>2</sub>L<sub>2</sub>] (dpgH<sub>2</sub> = diphenylglyoxime, L = CH<sub>3</sub>CN), by optical flash photolysis in the presence of the photosensitizer [Ru(bpy)<sub>3</sub>]<sup>2+</sup> and methyl viologen (MV<sup>2+</sup>) as the electron relay.<sup>[21]</sup> The latter oxidatively quenches the excited state of the photosensitizer and delivers the electron to the catalyst (Figure 1, top panel). In the absence of a sacrificial electron donor, charge recombination returns the system to its initial state. The solution structure of the Co<sup>I</sup> intermediate has been predicted using DFT,<sup>[17,20,22]</sup> but was never experimentally probed. A crystal structure of the Co<sup>I</sup> derivative [Co(dpgBF<sub>2</sub>)<sub>2</sub>(CH<sub>3</sub>CN)]<sup>-</sup> has been reported,<sup>[18]</sup> but the structure of the intermediate in solution can be significantly different from those in the solid phase. Here, we combine in situ time-resolved X-ray absorption near edge structure (XANES) spectroscopy and UV/Visible spectroscopy to investigate the early stages of hydrogen evolution mediated by **Co1** and **Co2** catalysts. We report the first experimental determination of the structure of the Co<sup>I</sup> intermediate formed from **Co2** in solution

[a] Dr. G. Smolentsev, Prof. J. A. van Bokhoven, Dr. M. Nachttegaal  
Paul Scherrer Institute, 5232 Villigen PSI (Switzerland)  
E-mail: grigory.smolentsev@psi.ch

[b] B. Cecconi, Dr. M. Chavarot-Kerlidou, Dr. V. Artero  
Laboratory of Chemistry and Biology of Metals  
Univ. Grenoble Alpes, CEA, CNRS, Grenoble (France)

[c] B. Cecconi  
Department of Materials Science and Milano-Bicocca Solar Energy  
Research Center, University of Milano-Bicocca, INSTM Unit  
20125 Milano (Italy)

[d] A. Guda  
International Research Center "Smart Materials"  
Southern Federal University, 344090 Rostov-on-Don (Russia)

[e] Prof. J. A. van Bokhoven  
Institute for Chemical and Bioengineering  
ETH Zurich, 8093 Zurich (Switzerland)

Supporting information for this article is available on the WWW under  
<http://dx.doi.org/10.1002/chem.201502900>.

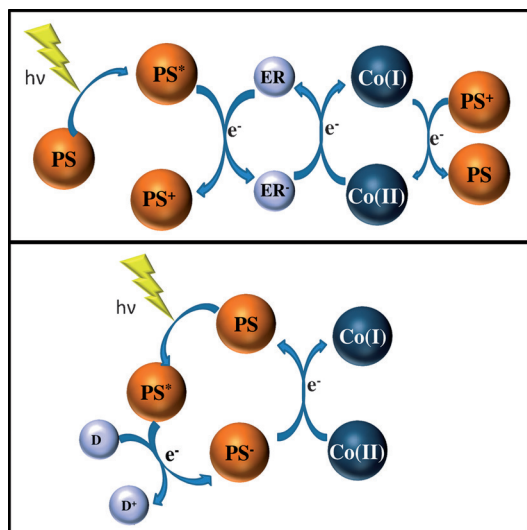


**Figure 1.** Two reaction pathways leading to the formation of  $\text{Co}^{\text{I}}$  intermediates. Top panel: transient formation of a  $\text{Co}^{\text{I}}$  intermediate in the presence of an electron relay (ER) followed by recombination with the oxidized photosensitizer (PS). Bottom panel: accumulation of  $\text{Co}^{\text{I}}$  species in the presence of a sacrificial electron donor (D).

and highlight a major difference in terms of reactivity and stability between  $\text{Co}^{\text{II}}$  and  $\text{Co}^{\text{I}}$  under photocatalytic conditions.

XANES spectra contain element-specific information about the structure of metal complexes.<sup>[23–25]</sup> Time-resolved X-ray absorption spectroscopy in the laser pump-X-ray probe mode was initially established for experiments in the picosecond–nanosecond time range.<sup>[26,27]</sup> We recently extended the technique to the microsecond range (pump-sequential-probe<sup>[28]</sup> and pump-flow-probe<sup>[29]</sup> methods, see the Supporting Information). These new setups coupled with state of the art simulations enables establishing the time-resolved XANES as a powerful tool to study the local structure of catalytic intermediates in light-driven reactions<sup>[23]</sup>.

The transiently formed  $\text{Co}^{\text{I}}$  intermediate (Figure 1, top) was monitored using time-resolved Co K-edge XANES. The sample consisted of  $\text{Co}^{\text{II}}$ ,  $[\text{Ru}(\text{bpy})_3]^{2+}$ , and  $\text{MV}^{2+}$  in acetonitrile.  $\text{NBu}_4\text{PF}_6$  (0.1 M) was added to control ion pairing and the ionic strength of the solution. A series of 200 Co K-edge XANES spectra corresponding to the time range (–50, 50)  $\mu\text{s}$  has been collected using the pump-sequential-probes method.<sup>[28]</sup> Analysis of these spectra using principal component analysis (PCA)<sup>[30,31]</sup> indicated that only one intermediate is present in this time series. This intermediate is formed within the first microsecond after the excitation of the photosensitizer. Figure 2 displays the spectrum of  $\text{Co}^{\text{II}}$  in its initial  $\text{Co}^{\text{II}}$  state (top panel) and the component corresponding to the transiently formed intermediate (bottom panel, .....). To access longer delays we performed the experiment on the same system using the pump-flow-probe method.<sup>[29]</sup> A similar transient signal was measured at 100  $\mu\text{s}$  delay (Figure 2, —). The positive signal of the transient XANES in the region of the rising edge (7715–7730 eV) is indicative of cobalt reduction. Thus  $\text{Co}^{\text{I}}$  is the only intermediate that is formed transiently in this multicomponent

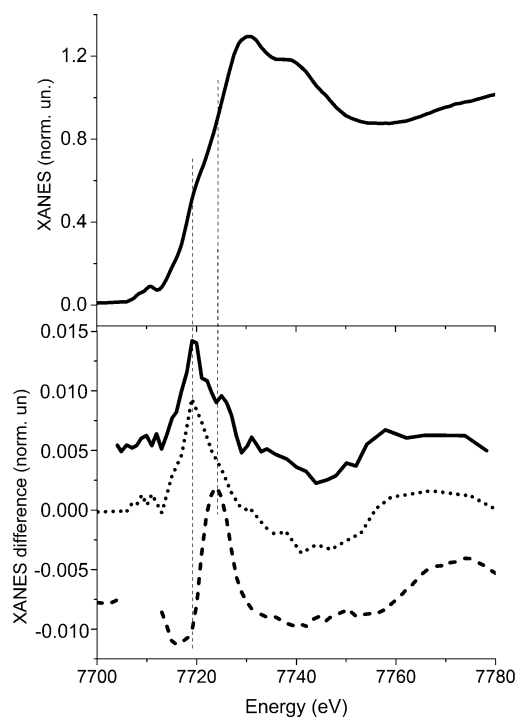


**Figure 2.** Top panel: Experimental Co K-edge XANES of the initial  $\text{Co}^{\text{II}}$  state of  $\text{Co}^{\text{II}}$  in acetonitrile. Bottom panel: Transient Co K-edge XANES spectrum corresponding to 100  $\mu\text{s}$  delay after laser excitation (—) of a  $[\text{Ru}(\text{bpy})_3]^{2+}/\text{MV}^{2+}/\text{Co}^{\text{II}}$  system in a pump-flow-probe setup; transient Co K-edge XANES extracted using PCA from the series of 200 spectra measured on the same system in the time range (–50, 50)  $\mu\text{s}$  (.....) with regard to the laser pulse in a pump-sequential-probe setup; the difference between the spectrum of the  $\text{Co}^{\text{I}}$  state accumulated for a system containing  $\text{Co}^{\text{I}}$  and Eosin Y in the presence of TEOA as the sacrificial electron donor and the corresponding spectrum of  $\text{Co}^{\text{II}}$  in acetonitrile (----). The spectrum obtained using the pump-flow-probe method was multiplied by 2.5 and shifted up, while the spectrum measured at accumulative conditions was divided by 21 and shifted down to simplify visual comparison.

system over the timeframe 0.5–100  $\mu\text{s}$ . The formation of a  $\text{Co}^{\text{III}}$  species<sup>[21]</sup> from the reaction of oxidized photosensitizer  $[\text{Ru}(\text{bpy})_3]^{3+}$  and  $\text{Co}^{\text{II}}$  was not observed.

Accumulation of  $\text{Co}^{\text{I}}$  in the presence of a sacrificial electron donor (Figure 1, bottom) has been monitored using in situ UV/Vis spectroscopy. The systems contained  $\text{CH}_3\text{CN}$  solutions of  $\text{Co}^{\text{II}}$ , triethanolamine (TEOA),  $[\text{Ir}(\text{ppy})_2(\text{bpy})]^+$  (ppy = phenylpyridine), or Eosin Y as the photosensitizer and  $\text{NBu}_4\text{PF}_6$  (0.1 M). The formation of the  $\text{Co}^{\text{I}}$  state of  $\text{Co}^{\text{II}}$  is evidenced by the characteristic two-band spectrum with maxima at 556 and 627 nm (Figure 3 and Figure S6 in the Supporting Information). The spectrum is in agreement with the references obtained for electro synthetically<sup>[32]</sup> and chemically reduced<sup>[19]</sup>  $\text{Co}^{\text{I}}$  derivatives of  $\text{Co}^{\text{II}}$  and with ab initio calculations.<sup>[22]</sup> Results are similar to those reported using a platinum-based photosensitizer<sup>[11]</sup> and to those observed in the microsecond range at transient conditions for  $[\text{Co}(\text{dpgBF}_2)_2(\text{CH}_3\text{CN})_2]$ .<sup>[21]</sup> Hydrogen is evolved under accumulation conditions which agrees with the previous report.<sup>[11]</sup> Thus  $\text{Co}^{\text{I}}$  intermediates of  $\text{Co}^{\text{II}}$  formed either transiently or under photoaccumulation conditions are identical and active for hydrogen evolution.

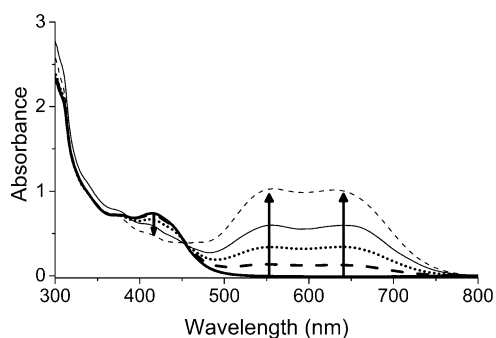


**Figure 3.** UV/visible spectra recorded before (thick solid line) and after 30 s (thick dash line), 1 min (dot line), 2.5 min (thin solid line) and 5 min (thin dash line) of visible light irradiation on anhydrous  $\text{CH}_3\text{CN}$  solutions of **Co2** and  $[\text{Ir}(\text{ppy})_2(\text{bpy})](\text{PF}_6)$  in the presence of TEOA (5%). The transition  $\text{Co}^{\text{II}} \rightarrow \text{Co}^{\text{I}}$  is outlined by the appearance of a two-component signal.

Theoretical modelling of the XANES spectra for **Co2** and the transiently formed  $\text{Co}^{\text{I}}$  intermediate allows the determination of their structure in solution. Two parameters were varied for **Co2**: the average distance between cobalt and nitrogen atoms in  $\text{dmg}^{2-}$  ligands (defined as rigid groups) and the bond length between cobalt and axial nitrogen atoms of the  $\text{CH}_3\text{CN}$  molecules. For the  $\text{Co}^{\text{I}}$  intermediate state we similarly varied the average distance between the cobalt center and nitrogen atoms of  $\text{dmg}^{2-}$  ligands and allowed variations in the distances between cobalt and axial ligands independently in opposite directions, that is, not excluding a transition from a six- towards a five-coordinated model. Additionally the displacement of the cobalt atom out of plane formed by nitrogen atoms of  $\text{dmg}^{2-}$  has been included into the model. The best simulated spectra for the  $\text{Co}^{\text{II}}$  and the  $\text{Co}^{\text{I}}$  species are compared with the experimental data in Figure 4. The model of  $\text{Co}^{\text{II}}$  is characterized by a  $\text{Co}-\text{N}(\text{dmg}^{2-})$  bond length of 1.86 Å, whereas the  $\text{Co}-\text{N}(\text{CH}_3\text{CN})$  distance is 2.02 Å. For the  $\text{Co}^{\text{I}}$  intermediate the best-fitted  $\text{Co}-\text{N}(\text{dmg}^{2-})$  bond length is 1.88 Å, the  $\text{Co}-\text{N}(\text{CH}_3\text{CN})$  lengths are 2.00 and 2.11 Å and the out of plane cobalt displacement is 0.08 Å. Thus, one of the axial bonds remains unchanged from the initial  $\text{Co}^{\text{II}}$  state while the other axial bond becomes slightly weaker. This model is thus at variance with previous DFT calculations for the  $\text{Co}^{\text{I}}$  state of **Co2**, in which the authors suggested either a four-<sup>[20]</sup> or five-coordinated<sup>[17]</sup> structure. It is also different from the five-coordinated structure of  $[\text{Co}(\text{dpgBF}_2)_2(\text{CH}_3\text{CN})_2]^-$  determined from single-crystal XRD.<sup>[18]</sup> Neither the full displacement of one axial ligand, nor the DFT-predicted significant (by  $\sim 0.2$  Å) shortening of one of the metal-solvent bonds has been observed upon reduction from  $\text{Co}^{\text{II}}$  to  $\text{Co}^{\text{I}}$ .<sup>[17,20]</sup>

We then investigated the other cobaloxime catalyst, **Co1**. We collected a Co K-edge XANES of the  $\text{Co}^{\text{I}}$  state accumulated in solution in the presence of a sacrificial electron donor (TEOA). Eosin Y was used as the photosensitizer. During the first minutes of light illumination, the spectrum of the initial  $\text{Co}^{\text{III}}$  complex evolved towards reduction and after approximately 15 min a stable signal was obtained. The absorption edge shifts to lower energies than in the  $\text{Co}^{\text{II}}$  state indicating a lower oxidation state of metal. The difference between the

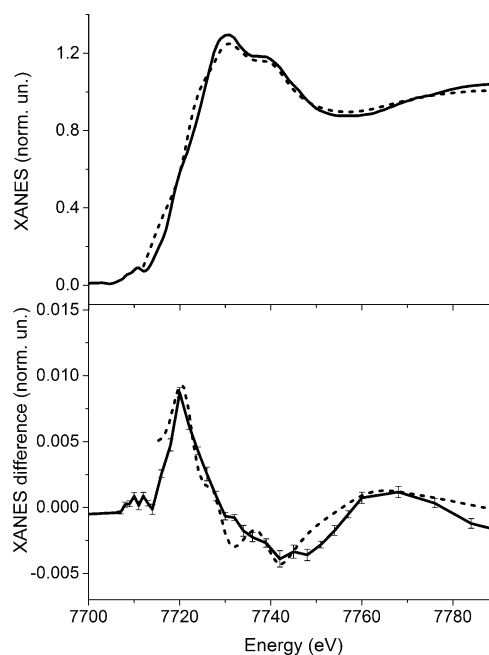


**Figure 4.** Top panel: Comparison of the experimental Co K-edge XANES of **Co2** in acetonitrile (—) with the theoretical simulation for the best-fit structure (----). Bottom: transient signal corresponding to the formation of a  $\text{Co}^{\text{I}}$  intermediate. Experimental (—) and theoretical calculations (----) for the best-fit model are shown.

spectrum obtained under these conditions and that of cobaloxime in the  $\text{Co}^{\text{II}}$  state is shown as (----) in the bottom panel of Figure 2. Its shape is significantly different from the transient signal observed in the time-resolved experiment using the **Co2** catalyst and assigned above to a  $\text{Co}^{\text{I}}$  intermediate. In particular the first positive peak is shifted by 5 eV to higher energies relative to the corresponding maximum of the time-resolved signal. This indicates that the structure of such an accumulated state is significantly different from that of the transiently formed  $\text{Co}^{\text{I}}$  intermediate.

UV/Vis monitoring of the same solution confirmed these observations. A transition from the  $\text{Co}^{\text{III}}$  to the  $\text{Co}^{\text{II}}$  state was first observed as a new absorption band at  $\sim 430$  nm, assigned to a d-d transition for the  $d^7$   $\text{Co}^{\text{II}}$  ion (Figures S7 and S8, Supporting Information). However neither typical signatures of the  $\text{Co}^{\text{I}}$  state nor the hydrogen evolution were observed upon longer irradiation. Further investigations indicated that water is required to observe both the typical signal of a  $\text{Co}^{\text{I}}$  intermediate and hydrogen evolution (Figure S9, Supporting Information, and previous reports<sup>[12,15]</sup>). Thus both Co K-edge XANES and UV/visible measurements indicate that the  $\text{Co}^{\text{I}}$  state accumulated during long-term irradiation in the presence of a sacrificial electron donor with **Co1** is different from the transiently formed  $\text{Co}^{\text{I}}$  intermediate observed with **Co2**.

The **Co1** and **Co2** systems differ by the bridge between oxime functions in the equatorial plane and by the presence of an axial pyridine ligand in **Co1**. To discriminate between these two differences, we prepared  $[\text{Co}(\text{dmgBF}_2)_2\text{pyCl}]$  (**Co3**) (synthesis is described in the Supporting Information) and monitored by UV/visible spectra under similar photocatalytic

conditions. A  $\text{Co}^{\text{I}}$  intermediate with two-band spectrum (identical to that observed for **Co2**) was found (Figure S10, Supporting Information). Pyridine is a stronger ligand than TEOA that excludes that a coordination bond between TEOA or its decomposition product and the cobalt could be responsible for the difference observed in the  $\text{Co}^{\text{I}}$  states in the above experiments. XANES spectra show such an interaction between sacrificial electron donor and **Co2** in the  $\text{Co}^{\text{II}}$  state (Figure S5, Supporting Information). However, the amplitude of the spectral changes at the rising edge of XANES (7715–7730 eV) is much smaller than the difference observed between the accumulated and transiently formed  $\text{Co}^{\text{I}}$  species at similar energies. The difference in behavior between **Co2** and **Co1** may thus be assigned to the nature of the bridge in the equatorial planes. Simulations indicate that the bridge between  $\text{dmg}^{2-}$  ligands does not influence the shape of XANES spectra significantly (Figure S4, Supporting Information) and therefore more severe modifications have to be found to explain this spectral difference.

Substituting the proton for  $\{\text{BF}_3\}$  bridges cathodically shifts the  $\text{Co}^{\text{III}}$  potential by 500 mV<sup>[33]</sup> and significantly increases the nucleophilicity of the  $\text{Co}^{\text{I}}$  center. We thus expected the  $\text{Co}^{\text{I}}$  intermediate of **Co1** to rapidly react with any source of protons in the medium, and specifically with the protons released by TEOA upon oxidation. Our data, however, show that this system is unable to evolve hydrogen, probably because of the limited amount of available protons and the quite basic conditions of the medium. Instead it may degrade through hydride transfer to the  $\text{dmgH}^-$  ligand.<sup>[34,35]</sup> Alternatively, the initial  $\text{Co}^{\text{I}}$  intermediate may react with an iminium species resulting from the decomposition of TEOA and generate a  $\text{Co}^{\text{III}}$ -alkyl species.<sup>[36]</sup> In both cases, the resulting  $\text{Co}^{\text{III}}$  species can be reduced to the  $\text{Co}^{\text{I}}$  state through light-driven electron transfers. However, due to the significant modification of their electronic structure, it is unlikely that the corresponding  $\text{Co}^{\text{I}}$  species exhibits absorption bands in the 550–650 nm region corresponding to transitions from a metal d orbital to  $\pi$  orbitals delocalized over imine bonds.<sup>[22]</sup> Such severe modifications are also in line with the major difference observed in the Co K-edge XANES spectrum (Figure 2) and the lack of hydrogen evolution activity observed for the accumulated  $\text{Co}^{\text{I}}$  state of **Co1**.

In conclusion, we presented the first structural determination of intermediates of photocatalytic systems observed in the microsecond range using time-resolved XANES. The solution structure of the  $\text{Co}^{\text{I}}$  intermediate of **Co2** indicates that only one axial solvent ligand of the cobalt center is labilized, but not fully displaced as it is observed in the solid state. While such a  $\text{Co}^{\text{I}}$  intermediate is the resting state of the **Co2**-based photocatalytic system, we showed that another catalytically inactive  $\text{Co}^{\text{I}}$  species forms under similar conditions when **Co1** is used as the catalytic platform. Further work can be focused on the other intermediates (in particular  $\text{Co}^{\text{III}}\text{H}$ ) of cobaloxime catalysts. The time-resolved XANES method that has been illustrated in this work can be generally applied to clarify the photocatalytic mechanism not only for hydrogen-evolving systems but also for other molecular photocatalysts.

## Acknowledgements

This work was supported by the Swiss National Science Foundation (grant no. 200021–135226), European Commission's Seventh Framework Programme (FP7/2007–2013) under grant agreement no. 290605 (COFUND: PSI-FELLOW) and ERC Grant Agreement no. 306398, the French National Research Agency (Labex program, ARCANÉ, ANR-11-LABX-0003-01), and Russian Foundation for Basic Research (project #14-02-31555). JAvB thanks the NCCR MUST. A.G. would like to thank Ministry of Education and Science of Russia (project #RFMEFI58714X0002). The COST Action CM1202 PERSPECT-H2O is also acknowledged.

**Keywords:** photocatalysis · solar fuels · transient X-ray absorption · XANES · X-ray absorption spectroscopy

- [1] V. Balzani, A. Credi, M. Venturi, *ChemSusChem* **2008**, *1*, 26–58.
- [2] A. Thapper, S. Styring, G. Saracco, A. W. Rutherford, B. Robert, A. Magnusson, W. Lubitz, A. Llobet, P. Kurz, A. Holzwarth, S. Fiechter, H. de Groot, S. Campagna, A. Braun, H. Bercegol, V. Artero, *Green* **2013**, *3*, 43–57.
- [3] J. R. McKone, S. C. Marinescu, B. S. Brunschwig, J. R. Winkler, H. B. Gray, *Chem. Sci.* **2014**, *5*, 865–878.
- [4] Z. Han, R. Eisenberg, *Acc. Chem. Res.* **2014**, *47*, 2537–2544.
- [5] V. S. Thoi, Y. Sun, J. R. Long, C. J. Chang, *Chem. Soc. Rev.* **2013**, *42*, 2388–2400.
- [6] P. Du, R. Eisenberg, *Energy Environ. Sci.* **2012**, *5*, 6012–6021.
- [7] V. Artero, M. Chavarot-Kerlidou, M. Fontecave, *Angew. Chem. Int. Ed.* **2011**, *50*, 7238–7266; *Angew. Chem.* **2011**, *123*, 7376–7405.
- [8] S. Losse, J. G. Vos, S. Rau, *Coord. Chem. Rev.* **2010**, *254*, 2492–2504.
- [9] J. L. Dempsey, B. S. Brunschwig, J. R. Winkler, H. B. Gray, *Acc. Chem. Res.* **2009**, *42*, 1995–2004.
- [10] A. Fihri, V. Artero, A. Pereira, M. Fontecave, *Dalton Trans.* **2008**, 5567–5569.
- [11] P. Du, J. Schneider, G. Luo, W. W. Brennessel, R. Eisenberg, *Inorg. Chem.* **2009**, *48*, 4952–4962.
- [12] P. Du, K. Knowles, R. Eisenberg, *J. Am. Chem. Soc.* **2008**, *130*, 12576–12577.
- [13] a) B. Probst, A. Rodenberg, M. Guttentag, P. Hamm, R. Alberto, *Inorg. Chem.* **2010**, *49*, 6453–6460; b) P. Zhang, M. Wang, J. Dong, X. Li, F. Wang, L. Wu, L. Sun, *J. Phys. Chem. C* **2010**, *114*, 15868–15874.
- [14] B. Probst, C. Kolano, P. Hamm, R. Alberto, *Inorg. Chem.* **2009**, *48*, 1836–1843.
- [15] R. S. Khnayzer, C. E. McCusker, B. S. Olaiya, F. N. Castellano, *J. Am. Chem. Soc.* **2013**, *135*, 14068–14070.
- [16] T. M. McCormick, B. D. Calitree, A. Orchard, N. D. Kraut, F. V. Bright, M. R. Detty, R. Eisenberg, *J. Am. Chem. Soc.* **2010**, *132*, 15480–15483.
- [17] B. H. Solis, S. Hammes-Schiffer, *Inorg. Chem.* **2011**, *50*, 11252–11262.
- [18] X. Hu, B. S. Brunschwig, J. C. Peters, *J. Am. Chem. Soc.* **2007**, *129*, 8988–8998.
- [19] J. L. Dempsey, J. R. Winkler, H. B. Gray, *J. Am. Chem. Soc.* **2010**, *132*, 16774–16776.
- [20] J. T. Muckerman, E. Fujita, *Chem. Commun.* **2011**, 47, 12456–12458.
- [21] J. L. Dempsey, J. R. Winkler, H. B. Gray, *J. Am. Chem. Soc.* **2010**, *132*, 1060–1065.
- [22] A. Bhattacharjee, M. Chavarot-Kerlidou, J. L. Dempsey, H. B. Gray, E. Fujita, J. T. Muckerman, M. Fontecave, V. Artero, G. M. Arantes, M. J. Field, *ChemPhysChem* **2014**, *15*, 2951–2958.
- [23] G. Smolentsev, V. Sundström, *Coord. Chem. Rev.* DOI: 10.1016/j.ccr.2015.03.001.
- [24] S. Bordiga, E. Groppo, G. Agostini, J. A. van Bokhoven, C. Lamberti, *Chem. Rev.* **2013**, *113*, 1736–1850.
- [25] R. Ortega, A. Carmona, I. Llorens, P. L. Solari, *J. Anal. At. Spectrom.* **2012**, *27*, 2054–2065.
- [26] C. Bressler, M. Chergui, *Annu. Rev. Phys. Chem.* **2010**, *61*, 263–282.

- [27] L. X. Chen, X. Zhang, J. V. Lockard, A. B. Stickrath, K. Attenkofer, G. Jennings, D. J. Liu, *Acta Crystallogr. Sect. A* **2010**, *66*, 240–251.
- [28] G. Smolentsev, A. A. Guda, M. Janousch, C. Frieh, G. Jud, F. Zamponi, M. Chavarot-Kerlidou, V. Artero, J. A. van Bokhoven, M. Nachttegaal, *Faraday Discuss.* **2014**, *171*, 259–273.
- [29] G. Smolentsev, A. Guda, X. Zhang, K. Haldrup, E. S. Andreiadis, M. Chavarot-Kerlidou, S. E. Canton, M. Nachttegaal, V. Artero, V. Sundstrom, *J. Phys. Chem. C* **2013**, *117*, 17367–17375.
- [30] G. Smolentsev, G. Guilera, M. Tromp, S. Pascarelli, A. V. Soldatov, *J. Chem. Phys.* **2009**, *130*, 174508.
- [31] E. R. Malinowski, *Factor Analysis in Chemistry*, Wiley, New York, **2002**.
- [32] D. P. Estes, D. C. Grills, J. R. Norton, *J. Am. Chem. Soc.* **2014**, *136*, 17362–17365.
- [33] C. Baffert, V. Artero, M. Fontecave, *Inorg. Chem.* **2007**, *46*, 1817–1824.
- [34] L. I. Simándi, É. Budó-Záhonyi, Z. Szeverényi, *Inorg. Nucl. Chem. Lett.* **1976**, *12*, 237–241.
- [35] L. I. Simándi, Z. Szeverényi, É. Budó-Záhonyi, *Inorg. Nucl. Chem. Lett.* **1975**, *11*, 773–777.
- [36] A. Rodenberg, M. Oraziotti, B. Probst, C. Bachmann, R. Alberto, K. K. Baldrige, P. Hamm, *Inorg. Chem.* **2014**, *53*, 646–657.

---

Received: July 23, 2015

Published online on September 4, 2015